Virology 379 (2008) 135–142

Contents lists available at ScienceDirect

Virology

journal homepage: www.elsevier.com/locate/yviro

Mapping the domain structure of the influenza A virus polymerase acidic protein (PA) and its interaction with the basic protein 1 (PB1) subunit

Tom S.Y. Guu [a], Liping Dong [a,1], Pernilla Wittung-Stafshede [a,b], Yizhi J. Tao [a,*]

[a] Department of Biochemistry and Cell Biology, MS-140, Rice University, Houston, Texas 77005, USA
[b] Department of Chemistry, Rice University, Houston, Texas 77005, USA

ARTICLE INFO

Article history:
Received 16 April 2008
Returned to author for revision 13 June 2008
Accepted 17 June 2008
Available online 26 July 2008

Keywords:
Influenza
Polymerase
PA
PB1

ABSTRACT

The influenza A virus polymerase consists of three subunits (PA, PB1, and PB2) necessary for viral RNA synthesis. The heterotrimeric polymerase complex forms through PA interacting with PB1 and PB1 interacting with PB2. PA has been shown to play critical roles in the assembly, catalysis, and nuclear localization of the polymerase. To probe the structure of PA, we isolated recombinant PA from insect cells. Limited proteolysis revealed that PA contained two domains connected by a 20-residue linker (residues 257–276). Far-UV circular dichroism established that the two domains folded into a mixed α/β structure when separately expressed. *In vitro* pull-down assays showed that neither individually nor cooperatively expressed PA domains, without the linker, could assure PA–PB1 interaction. Protease treatment of PA–PB1 complex indicated that its PA subunit was significantly more stable than free PA, suggesting that the linker is protected and it constitutes an essential component of the PA–PB1 interface.

Introduction

The influenza A virus, a family *Orthomyxoviridae* pathogen of mammals and birds, contains eight negative-sense RNAs that encode eleven proteins (Chen et al., 2001; Whittaker, 2001). The influenza RNA-dependent RNA polymerase consists of three subunits (PA, PB1, and PB2) responsible for viral replication and transcription. During replication, a negative-sense vRNA acts as a template for the synthesis of a non-polyadenylated, positive-sense cRNA. This cRNA is subsequently used to generate negative-sense vRNA progeny. Although viral replication is primer-independent, initiation of viral transcription requires a capped mRNA fragment primer (Lamb and Krug, 2001).

Various accounts of the necessary minimal composition for a functional polymerase complex capable of synthesizing vRNA, cRNA, and mRNA have been reported over the years. It was reported that PB1 alone could transcribe RNA template *in vitro* (Kobayashi et al., 1996) and could catalyze cRNA synthesis (Nakagawa et al., 1996). Others showed that the PB1–PB2 complex exhibited catalytic properties similar to those of the PA–PB1–PB2 complex, while the PA–PB1 complex was able to initiate *de novo* (*i.e.*, primer-independent) RNA synthesis, suggesting that the catalytic specificity of the PB1 subunit was modulated to transcriptase or to replicase by binding to PB2 or PA, respectively (Honda et al., 2002). In contrast, other findings indicated that PB2 was essential for both primer-dependent and *de novo* initiation (Deng et al., 2005; Lee et al., 2002). Still, some PA mutants impaired the ability of the polymerase complex to synthesize mRNA, cRNA, and vRNA, implying that PA played a critical role in both transcription and replication (Fodor et al., 2002). It is now widely accepted that all three polymerase subunits are required for the synthesis of vRNA, cRNA and mRNA.

Specific functions have been assigned to the PB1 and PB2 subunits of the heterotrimeric polymerase complex. PB1 contains the S-D-D motif characteristic of RNA-dependent RNA polymerases and is the catalytic site for RNA synthesis (Argos, 1988; Biswas and Nayak, 1994; Braam et al., 1983). Indeed, the binding sites for 5′- and 3′-vRNA and cRNA are located on the PB1 subunit (Fodor et al., 1993; Gonzalez and Ortin, 1999; Li et al., 1998). And although PB1 possesses the endonuclease activity required to snatch capped primers from host mRNA to initiate transcription (Li et al., 2001), PB2 is responsible for binding to the cap structure of the host mRNA (Fechter et al., 2003; Li et al., 2001). Unlike PB1 and PB2, the role of PA in viral replication and transcription is not well defined.

Many genetic studies have investigated the functions of PA. For example, an R638A mutation resulted in the generation of defective interfering RNA, implying that PA could act as an elongation factor (Fodor et al., 2003). An H510A mutation resulted in negligible transcriptional activity, while viral replication was unaffected. *In vitro* analysis of the recombinant polymerase carrying a PA H510A mutation revealed that the endonuclease activity of the polymerase was severely impaired (Fodor et al., 2002). In addition, three other residues were later identified to be involved in cap binding (K102) and endonuclease activities (D108 and K134) (Hara et al., 2006). These findings suggest the possible involvement of PA in the endonuclease cleavage of cellular pre-mRNA, an initial step in viral transcription. In

* Corresponding author. Fax: +1 713 348 5154.
E-mail address: ytao@rice.edu (Y.J. Tao).
[1] Present address: Department of Pathology, Baylor College of Medicine, Houston, Texas 77030, USA.

0042-6822/$ – see front matter © 2008 Elsevier Inc. All rights reserved.
doi:10.1016/j.virol.2008.06.022

addition, a T157A mutation also resulted in several defects, including delayed transport of PA to the nucleus and reduced replication activity, especially cRNA synthesis, while the transcription activity was unaltered (Huarte et al., 2003). The mutation of PA residues G507A and R508A resulted in the production of non-infectious viral particles, although there was little effect on transcription or replication (Regan et al., 2006). Moreover, studies have shown that PA was involved not only in the assembly of a functional viral RNA polymerase complex (Kawaguchi et al., 2005), but also in the assembly and release of influenza virions (Regan et al., 2006). PA seemingly has broad effects on polymerase activities, although its mechanistic underpinnings are not clearly understood.

PA also exhibits nuclear transport and proteolytic activities. Its N-terminal region (residues 1–256) contains nuclear localization signals (NLS), which direct the transport of PB1 from the cytoplasm to the nucleus (Nieto et al., 1994). It has also been noted that over-expression of PA in mammalian and insect cells induced the degradation of PB2 and NP, implying that PA may function as a protease (Sanz-Ezquerro et al., 1995). Indeed, Hara et al. established PA as a serine protease (exhibiting chymotrypsin-like activity) with an active site located at S624 (2001). However, Sanz-Ezquerro et al. reported that the first 257 amino acid residues were responsible for the proteolytic activity of PA (1996). Perales et al. linked PA-mediated induction of proteolysis to the replication activity of the polymerase complex (2000), yet Naffakh et al. reported otherwise (2001). Lastly, phosphorylated isoforms of PA were observed (Sanz-Ezquerro et al., 1998). However, whether this post-translational modification of PA plays a role in its protease activity or in the RNA synthesis of the polymerase complex remains unclear.

A crystal structure of the polymerase complex or its subunits has yet to be elucidated. The only available three-dimensional structure of the polymerase complex, determined by electron microscopy to 23-Å resolution, shows a compact structure with no apparent boundaries between subunits (Area et al., 2004). Efforts have been undertaken to dissect the molecular anatomy of the polymerase complex. Current wisdom holds that inter-subunit interaction occurs linearly: the C-terminal region of PA binds to the N-terminal region of PB1, and the C-terminal region of PB1 binds to the N-terminal region of PB2 (Gonzalez et al., 1996; Ohtsu et al., 2002; Toyoda et al., 1996; Zurcher et al., 1996). Earlier mutagenesis studies have implicated the C-terminal two thirds of PA in PB1 binding, whereas the first 154 N-terminal amino acids appeared to be dispensable (Toyoda et al., 1996; Zurcher et al., 1996). Meanwhile, other studies have reported that the length of the N-terminal region of PB1 involved in PA binding ranges from the first 140 to the first essential 12 residues constituting the core of the interaction interface (Ohtsu et al., 2002; Perez and Donis, 1995, 2001; Toyoda et al., 1996). Recently, Ghanem et al. demonstrated that a 25-residue peptide corresponding to the PA binding domain of PB1 was capable of abolishing the polymerase activities of the virus and of suppressing viral growth (2007).

The objective of our study was to map the structural domains of PA and their functional roles in polymerase assembly using biochemical and biophysical techniques. Our results show that PA consists of two domains (residues 1–256 and 277–716, respectively) connected by a flexible linker. The linker region is buried at the PA–PB1 interface, and neither domain individually or collectively is sufficient for the formation of a stable PA–PB1 complex in the absence of the linker.

Results

PA domain determination by limited protease digestion

We successfully expressed influenza virus polymerase acidic protein (PA) of influenza A/PR/8/34 in insect cells using a baculovirus expression system. Using Ni-NTA affinity, heparin affinity, gel filtration, and anion exchange chromatography, recombinant PA was purified to 95% purity, as judged by Coomassie SDS-PAGE (Fig. 1A, lane 1). PA has 716 amino acids, corresponding to a molecular weight of 83 kD. PA eluted from the Superdex 200 gel filtration column at the

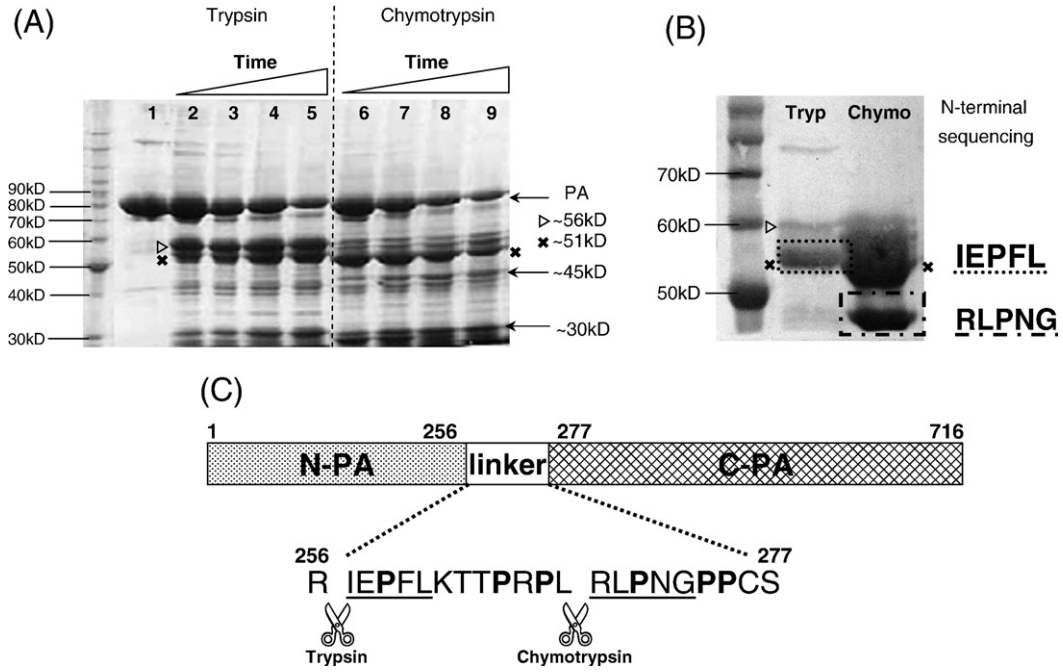

Fig. 1. Domain determination and identification of the influenza PA subunit. (A) Limited protease digestion of PA by trypsin and chymotrypsin. Purified PA (1.5 mg/ml, L1) was digested by trypsin (0.002 mg/ml) and chymotrypsin (0.006 mg/ml) at 20 °C for various lengths of time (3, 7, 15, and 25 min corresponding to L2–L5 or L6–L9). Digested PA samples were resolved by 9% SDS-PAGE stained with Coomassie blue. Major fragments are labeled with arrows (undigested PA, 45 and 30 kD) or symbols (56 and 51 kD) and corresponding sizes. (B) Digested PA fragments for N-terminal sequencing. Two bands, one of chymotrypsin (~45 kD) and one of trypsin (~51 kD), were selected for N-terminal sequencing, the result of which is shown on the right and labeled with dashed rectangular boxes and lines. (C) Schematic diagram of PA. PA contains two major domains, one from residues 1 to 256 (*i.e.*, N-PA) and one from residues 277 to 716 (*i.e.*, C-PA). The zoom-in linker region displays all 20 amino acids from residues 257 to 277. N-terminal sequencing results are underlined and protease cleavage sites are marked. Prolines within the linker region are shown in bold.

~80 kD position (Fig. 2), suggesting that PA assumed a monomeric state in the absence of other polymerase protein subunits. We estimated that approximately 0.25 mg of PA protein could be purified from 1 l of insect cell culture.

Limited proteolysis is an important tool for gaining information on domain arrangements and flexible structural parts of large proteins for which no NMR or crystal structures exist. To map the domain structure of PA, samples of PA were subjected to limited protease digestion using both trypsin and chymotrypsin in separate experiments. Under 750:1 PA-to-trypsin and 250:1 PA-to-chymotrypsin mass ratios, certain fragments appeared and grew stronger in intensity with increasing digestion time. The fragments of PA were of similar sizes regardless of the protease used; bands appeared at ~56, ~51, ~43 and ~30 kD for trypsin, and at ~51, ~45 and ~30 kD for chymotrypsin (Fig. 1A). Similar digestion patterns were also observed when PA samples of the A/Udorn/72 and A/HK/97 strains were treated with trypsin and chymotrypsin (data not shown). An earlier study on PA from the A/Puerto Rico/8/34 strain reported similar findings (Hara et al., 2006). The observation of persistent PA fragments from limited proteolysis suggested the presence of one or more flexible and exposed structural loops that connect polypeptide regions and may directly interact with one another in a folded state.

Next we determined the identities of the PA fragments by performing similar proteolysis experiments on N-His-tagged PA. The digested PA samples were subjected to a His-Trap affinity column. The results showed that the ~30 kD fragment was able to bind to the His-Trap resin while the ~51 kD and the ~45 kD bands were not. This observation suggested that the proteases cleaved PA into two domains, the N-terminal ~30 kD domain and the C-terminal ~45/51 kD domain. The more stable ~51 kD PA fragment (compared to the upper ~56 kD counterpart) from trypsin digestion and the ~45 kD PA fragment from chymotrypsin digestion were submitted for N-terminal sequencing (Fig. 1B). Sequencing results showed that the trypsin cleavage site was located at residues 256/257 and that the chymotrypsin cleavage site was at residues 268/269. A closer look at the sequence between amino acids 250–280 revealed a high percentage of proline residues (a total of six) in that region. Thus, we hypothesized that PA consisted of two major domains, one of 30 kD (amino acids 1–256) and one of 51 kD (amino acid 277–716), connected by a linker region (amino acids 257–277) that was largely flexible and exposed (Fig. 1C). The rationales behind the designations of the domain boundaries and linker region are considered in the Discussion section. Indeed, both trypsin and chymotrypsin digestion of the C-His tagged PA showed that the 51 kD fragment had an intact His-tag (anti-His panel of Fig. 6). Although a minor cleavage site near the C-terminus was occasionally observed for chymotrypsin which further reduced the 51 kD fragment into a 45 kD one, prolonged protease digestion of PA produced only two major truncated fragments of 30 and 51 kD (data not shown), consistent with our two-domain hypothesis. For clarity, in this text, the domain encompassing amino acids 1–256 will be referred to as N-PA and that of amino acids 277–716 as C-PA.

Expression, purification, and biophysical characterization of PA domains

In order to further characterize the two domains of PA, we developed an expression and purification protocol to obtain pure protein samples of both domains. As we did with PA, we sub-cloned N-PA and C-PA into pFastbac1 plasmids with 6× C-terminal His-tags. The domains were expressed separately in insect cells and purification steps similar to those used for PA were employed. Both N-PA and C-PA were eluted at the expected molecular weights from a Superdex 200 size-exclusion column. Their purity was comparable to that of PA (Fig. 2).

Once pure N-PA and C-PA were obtained, we assessed the structural integrity of the domains by far-UV CD spectroscopy, a method for evaluating protein secondary structure. In order to minimize background noise, we used a simple buffer of 10 mM potassium phosphate and 10 mM sodium chloride, pH 7.5. Both PA and the two individual domains were soluble in this buffer. Comparative control experiments of the proteins in different buffers implied structural integrity in each case regardless of the buffer used (data not shown). The far-UV CD spectra in the 195–250 nm range with two negative maxima at 208 and 222 nm indicated that the PA, N-PA, and C-PA were properly folded and contained mostly α helical content (Fig. 3). Secondary structure prediction based on the CD spectra revealed that all three proteins contained a mix of α- and β-structure along with some unordered regions (Table 1). Interestingly, when the experimental CD spectra of N-PA and C-PA were added together, the sum closely matched the experimental spectrum of PA (Fig. 3). This result suggests that the individual domains adopt conformations similar to their structures in the full-length protein, further supporting our conclusion that PA consists of two independently folded domains.

Interaction between the two domains of PA

To test whether the two separate domains interact with each other upon mixing, separately purified C-PA and N-PA were incubated

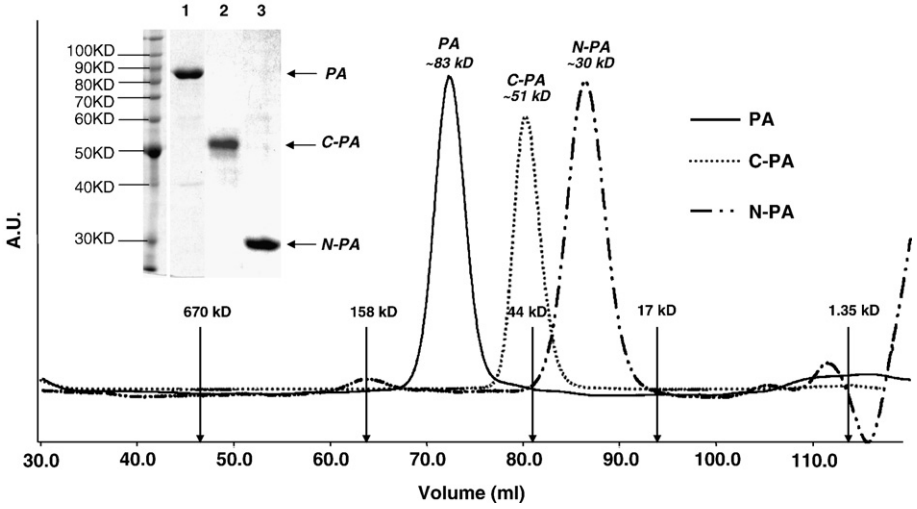

Fig. 2. Gel-filtration chromatogram of purified PA and the two individual major domains. PA, C-PA, and N-PA eluted from a Superdex size-exclusion column are marked by size. The peak positions of protein standards are also indicated. Purified PA (L1), C-PA (L2), and N-PA (L3) were resolved by 10% SDS-PAGE stained with Coomassie blue, as shown in the upper left corner. The proteins, originally resolved on separate SDS-PAGE, are aligned by size.

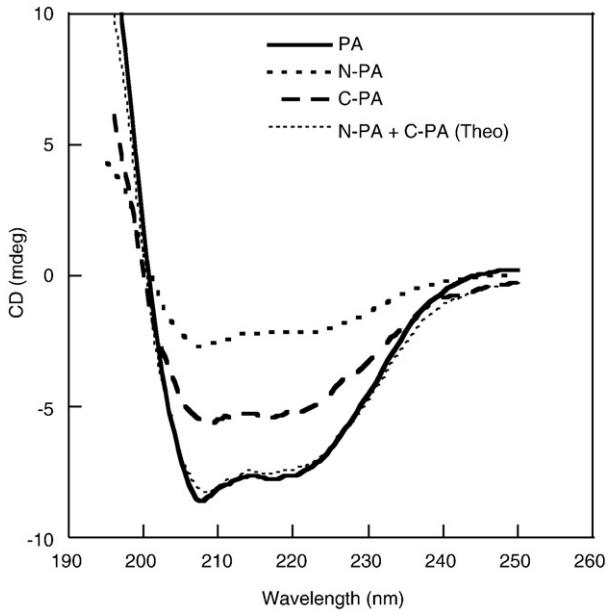

Fig. 3. Far-UV CD Spectra of PA and its two domains. The secondary structure of purified PA, C-PA, and N-PA (all at 1 μM) was probed in the 195–250 nm range. Protein buffer was 10 mM potassium phosphate and 10 mM sodium chloride, pH 7.5, 20 °C.

together (2.13 μM C-PA, 3.2 μM N-PA, 20 °C, 1 h) and loaded on a Superdex 200 gel filtration column. However, no complex eluted at the position of PA (*i.e.*, at 72 ml); instead, C-PA and N-PA eluted at the volumes corresponding to the individual domains (80 ml for C-PA, 87 ml for N-PA) (data not shown). Similar results were observed on the Superose12 gel filtration column, even when higher concentrations of C-PA and N-PA were used in the mixture (16 μM C-PA, 24 μM N-PA). We also co-expressed both PA domains by co-infecting insect cells with C-PA and N-PA recombinant baculoviruses. However, size-exclusion chromatography revealed that C-PA and N-PA did not interact with each other even when expressed simultaneously.

Thermal stability of PA and individual domains

We investigated the thermal stability of PA, C-PA, and N-PA using far-UV CD. Upon protein denaturation, the negative CD signal at 220 nm decreases towards zero, indicating an unfolded polypeptide. We found that thermal denaturation of all three proteins was irreversible; cooling of the samples after heating did not result in recovery of native-like CD signals. The proteins likely aggregated upon unfolding, causing the process to be irreversible. This phenomenon is common for large or cysteine-rich proteins; indeed, C-PA and N-PA have 10 and 4 cysteines, respectively. At high temperatures, cysteines readily oxidize to sulfonic acid or crosslink to form disulfides. Our attempts to overcome this problem by testing a range of buffers and additives were unsuccessful. To facilitate comparison of the thermal resistance among the proteins, experiments were conducted at identical heating rates. Because of this fact, thermal mid-points (T_m) are of only relative value. At identical conditions, the T_m for N-PA was 46 °C and the T_m for C-PA was 61 °C (pH 7.5, 0.5 °C/min). Both protein domains unfolded in cooperative processes, evident from their sigmoidal thermal profiles (Fig. 4). The thermal profile of PA involved a broad transition, much like that for C-PA. In summary, N-PA was less thermally resistant than C-PA, but appeared to be stabilized by the rest of PA.

Table 1
Prediction of PA, N-PA, and C-PA secondary structure

Protein	α-Helix	β-Strand	Turn	Unordered
PA	36%	18%	19%	28%
N-PA	33%	20%	19%	27%
C-PA	38%	17%	19%	28%

Secondary structure prediction based on the CD spectra of PA and the two PA domains using the CDSSTR program at DICHROWEB (http://www.cryst.bbk.ac.uk/cdweb/html/).

Characterization of the interaction of PA and its two domains with PB1

Although PA does not exhibit any well-characterized biochemical activities, it is indispensable for the transcription and replication activity of the influenza polymerase (Fodor and Smith, 2004; Honda et al., 2002; Nakagawa et al., 1996). PA has been shown to directly interact with PB1 but not PB2 in the assembly of the polymerase complex. Several mutagenesis studies have shown that extensive polypeptide regions of PA are required for PA–PB1 interaction, except the first 154 N-terminal residues of PA (Toyoda et al., 1996; Zurcher et al., 1996). To assess the role of these two PA domains in PA–PB1 complex formation, we performed a pull-down assay by co-infecting insect cells with different combinations of PA, C-PA, N-PA, and PB1 recombinant baculoviruses (Fig. 5A). All of our PA-related constructs contained a His-tag to facilitate complex detection. The soluble portion of the cell lysate of the different combinations was subjected to Ni-NTA affinity column. Anti-His antibody was used to assess the presence of PA, C-PA, and N-PA, whereas anti-PB1 was used to detect recombinant PB1 in the eluted fractions. With a C-terminal His-tag, PA, C-PA, and N-PA bound to the Ni-NTA resins and were eluted with high concentrations of imidazole. Our anti-His Western blot confirmed the presence of the PA, C-PA alone, N-PA alone, and C-PA and N-PA (Fig. 5B, top panel) in four separate experiments. PB1, however, co-eluted only with PA. Neither C-PA or N-PA alone, nor co-expression of the two domains, was found to form a stable complex with PB1 (Fig. 5B, bottom panel). Pull-down assays were repeated four times with similar results. It is also important to note that the presence of the 6× His-tag at either terminus of PA did not interfere with the assembly of the PA–PB1 complex and that the concentration of imidazole had no effect on PA–PB1 complex formation (data not shown). Our findings

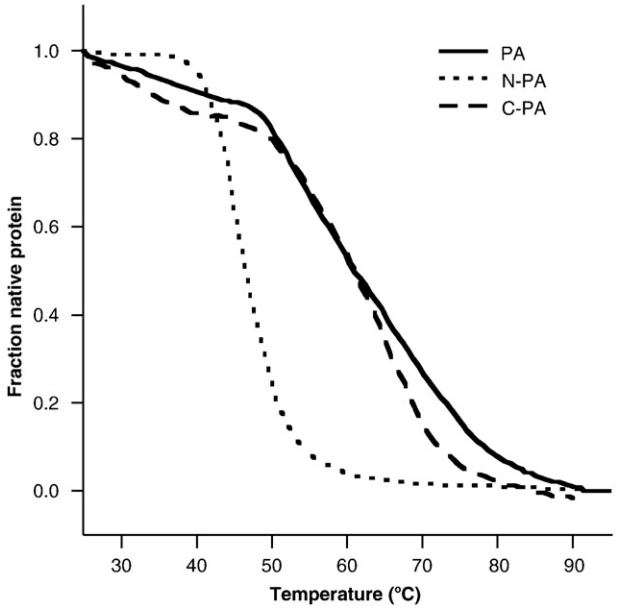

Fig. 4. Thermal denaturation of PA and its two domains. PA, C-PA, and N-PA were subjected to slow heating. Relative change in CD signal at 220 nm was monitored as a function of temperature. The signals were normalized, with 1 being the native protein signal at 25 °C and 0 being the signal of the denatured protein at 95 °C. All thermal experiments were performed in a buffer of 50 mM potassium phosphate and 200 mM sodium chloride, pH 7.5, and at a heating rate of 0.5 °C/min. The starting temperature was 25 °C. CD data were collected every 0.5 °C until 95 °C.

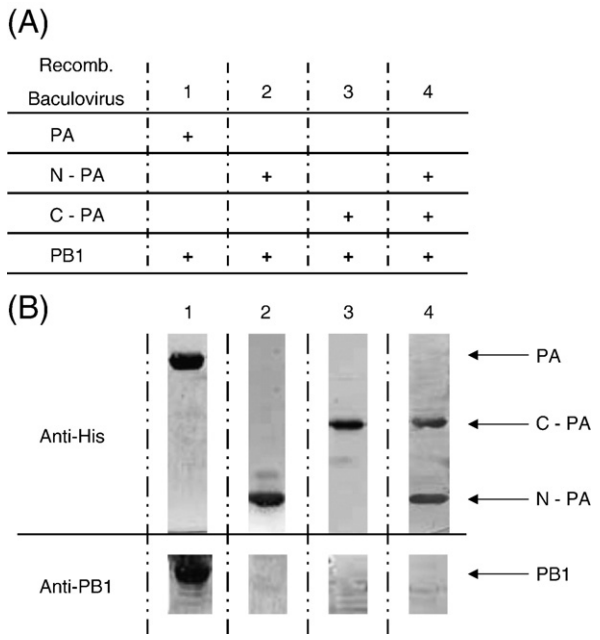

Fig. 5. Pull-down assay. (A) Different combinations of recombinant baculovirus co-infection. Insect cells were infected by: (1) PA and PB1 baculovirus; (2) N-PA and PB1 baculovirus; (3) C-PA and PB1 baculovirus; and (4) N-PA, C-PA, and PB1 baculovirus, at a multiplicity of infection (MOI) of 5. Infected cells were harvested 48 h post-infection. (B) Western blot of the eluted fraction. Infected insect cells were lysed and separated by centrifugation. Supernatant was incubated with Ni-NTA resins for 1 h at 4 °C. Flowthrough, wash, and eluted fractions from the Ni-NTA affinity column were collected. Anti-His antibody recognized the six His-tags located at the C-terminus of PA, C-PA, and N-PA (top panel). An anti-PB1 polyserum was used to detect any co-eluted PB1. Positions of PA, C-PA, N-PA, and PB1 on the PVDF membrane are marked by arrows. The proteins, originally resolved on separate PVDF membranes, are aligned by size.

thus suggested that the PA linker region (residues 257–276) was required for PA–PB1 interaction.

Limited protease digestion of the PA–PB1 complex

To probe the domain structure of PA upon interaction with PB1, we treated purified PA–PB1 complex with trypsin and chymotrypsin as we had done with PA. As described in the Materials and methods section, PA–PB1 complex was obtained by co-expression using the baculovirus expression system. A 6× His-tag was added at the C-terminus of PA to facilitate purification and identification of digested peptides. The PA–PB1 complex was purified using Ni-NTA affinity, heparin affinity, gel filtration, and cation exchange chromatography. PA–PB1 presumably formed a 1:1 complex as the two subunits had equal intensities on SDS-PAGE. Approximately 0.08 mg of PA–PB1 complex can be isolated from one liter of insect cell culture.

Surprisingly, we found that PA complexed with PB1 was highly resistant to protease digestion. In comparison, PB1 was quickly degraded even before the level of PA had undergone noticeable changes (Fig. 6). To facilitate PA peptide identification, digested proteins were subjected to Western blot analysis using an anti-His antibody. Since both the free PA and PA–PB1 complex contained a His-tag at the C-terminus of PA, only C-terminal PA fragments were detected (Fig. 6). Our results showed that nearly 90% of the PA in the PA–PB1 complex remained intact after 1 h of chymotrypsin digestion (250:1 PA-to-chymotrypsin, 20 °C) (Fig. 6A, lane 12). Under the same conditions, only ~10% of free PA was left intact, with emergence of truncated C-PA (Fig. 6A, lane 5). As PB1 was digested by prolonged chymotrypsin digestion (2 h and beyond), increasing amounts of C-PA appeared as the result of protease digestion of PA (Fig. 6A, lane 13 and 14). Similar results were also observed for trypsin digestion (750:1 PA-to-trypsin, 20 °C) (Fig. 6B). Therefore, the PA flexible linker region,

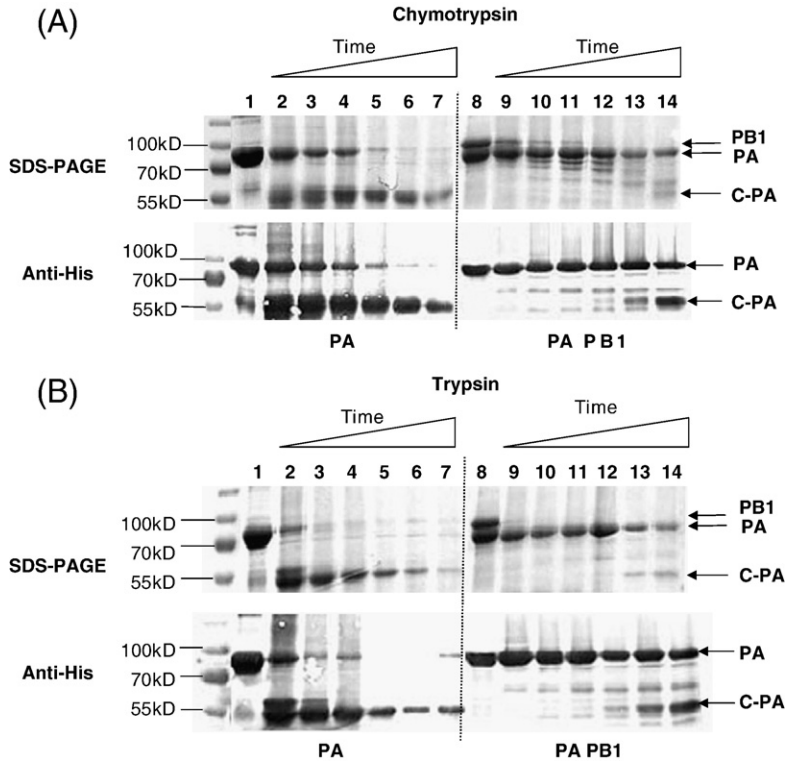

Fig. 6. Protease digestion pattern of free PA versus PA–PB1 complex. (A) and (B) SDS-PAGE (top panel) and Western blot (bottom panel) of limited proteolysis of PA (left) and the PA–PB1 complex (right) by chymotrypsin and trypsin. Purified PA (1.5 mg/ml, L1) and PB1 (1.5 mg/ml, L8) were digested by chymotrypsin (0.006 mg/ml) and trypsin (0.002 mg/ml) at 20 °C for various lengths of time (10 min, 20 min, 40 min, 1 h, 2 h, and 4 h, corresponding to L2–L7 and L9–L14). Digested PA–PB1 samples were resolved by 10% SDS-PAGE and transferred to PVDF membrane. Anti-His antibody was used to recognize the six His-tags located at the C-terminus of PA. PB1, PA and truncated C-PA are labeled with arrows.

readily accessible for protease digestion in free PA, was likely buried at the interface with PB1. The distinct protease digestion patterns of the PA–PB1 complex and the free PA corroborated the findings of our pull-down assay — that the PA linker (residues 257–276) constituted part of the PA–PB1 interface.

Discussion

Although many genetic studies have investigated the role of PA in influenza virus transcription and replication (Fodor et al., 2002, 2003; Huarte et al., 2003; Naffakh et al., 2001; Perales et al., 2000), little is known about the biophysical and structural properties of PA. In the absence of a crystal structure, we have used a set of biochemical and biophysical techniques in combination with purified protein variants to analyze the domain structure of PA and the functional roles of different PA domains in mediating PA–PB1 interaction. Based on the digestion pattern of PA by chymotrypsin and trypsin, we conclude that PA consists of two major domains (residues 1–256 and 277–716), connected by a 20-residue linker. A similar model was proposed by Hara et al. based on trypsin digestion (2006). Their results suggested a domain spanning residues 1 to 212 and another from residues 212 to the C-terminus, albeit no further domain characterization was performed. Like Hara et al., we also observe 25 and 56 kD fragments (residues 1–212 and 213–716, respectively) during trypsin digestion. However, only the 30 and 51 kD bands are the *common* dominant fragments following prolonged trypsin and chymotrypsin digestions. Nearly all secondary structure prediction programs we have explored, SSPro 3/8 (Pollastri et al., 2002), PSIPRED (Jones, 1999), Porter (Pollastri and McLysaght, 2005), APSSP2 (Raghava, 2002) and Jufo (Meiler and Baker, 2003; Meiler et al., 2001), indicate that the residues 257–277 have a high propensity for loop formation and are preceded and followed by helical structures. In addition, inter-domain linker prediction programs, such as DomCut (Suyama and Ohara, 2003) and DLP-SVM (Miyazaki et al., 2002; Tanaka et al., 2006), agree that residues 250–280 likely comprise the linker region of PA. By considering together our protease digestion patterns, N-terminal sequencing results, and computational predictions, we have arrived at our designations of the domain/linker boundaries of PA. Nevertheless, we recognize that our domain/linker designations might be imprecise; indeed, they could vary by ~5–10 residues depending on the availability of specific protease cleavage sites.

Herein we confirm the presence of two PA domains by the expression, purification, and characterization of the domains individually. Far-UV CD spectra of C-PA and N-PA demonstrate that these two domains are properly folded independent of each other with secondary structural content matching that of PA. Agreement between the theoretical sum of the CD signals of the two domains and the experimental signal of PA suggests that little conformational change occurs in the two domains in the absence of the linker region. These results validate our two-domain hypothesis and our choice of domain/linker boundaries. In addition, our binding experiments using gel filtration chromatography fail to detect any interaction between C-PA and N-PA It does, however, remain possible that the two domains could have some weak interactions in the full-length PA, as the flexible linker may function to bring the two domains together, thus facilitating their interactions *in vivo.*

Previous studies have mapped the interaction sites of the three subunits of the influenza virus polymerase. The C-terminal region of PA binds to the N-terminal region of PB1 and the C-terminal region of PB1 binds to the N-terminal region of PB2 (Gonzalez et al., 1996; Ohtsu et al., 2002; Toyoda et al., 1996; Zurcher et al., 1996). For PA–PB1 interaction, the PA binding site on PB1 was first identified to involve residues in the N-terminal region of PB1 (Gonzalez et al., 1996; Toyoda et al., 1996). The subsequent refined map narrowed the PA binding region from the first 140 amino acids to 48, 25, and eventually the first 12 residues constituting the core of the interaction interface (Ohtsu et al., 2002; Perez and Donis, 1995, 2001; Toyoda et al., 1996). In contrast, the PB1-interacting interface of PA appears to be more extensive. Several studies have indicated that essential interface regions are widely spread along the PA sequence, although it has been determined that the first 154 residues are not needed for PB1 interaction (Toyoda et al., 1996; Zurcher et al., 1996).

Our study therefore addresses PA–PB1 interaction in light of the two-domain structure of PA. Our pull-down assay indicates that neither domain alone nor a combination of the two domains, without the PA linker, is sufficient to bind PB1. Our limited proteolysis of the PA–PB1 complex shows that PA becomes highly resistant to both chymotrypsin and trypsin digestion, likely because the PA linker region is protected from protease digestion when complexed with PB1. By incorporating previously published data with our own findings, we have arrived at a model of PA–PB1 assembly (Fig. 7). This model favors an extensive interaction between C-PA and PB1 (Gonzalez et al., 1996; Ohtsu et al., 2002; Toyoda et al., 1996; Zurcher et al., 1996) and limited contact between N-PA and PB1 (Toyoda et al., 1996; Zurcher et al., 1996), with the linker buried at the PA–PB1 interaction interface. The linker region may function in PA–PB1 assembly via two possible scenarios. First, the linker may simply act as a passive inter-domain bridge, bringing together both PA domains to ensure PA–PB1 assembly. Second, the linker might be involved in a sequence specific interaction with PB1. Further experiments are required to determine the exact role of the linker in terms of PA–PB1 interaction. Furthermore, although N-PA and C-PA, individually or collectively, possess similar secondary structure content as full-length PA, it remains possible that the tertiary structure of the two domains could be different when individually expressed. Such a difference may interfere with the complex formation with PB1.

The role of PB2 in polymerase assembly is beyond the scope of this study and is therefore not described here. This is partly because purifying large amounts of the viral heterotrimeric polymerase is difficult, and also because of the insolubility of PB2 when separately expressed in insect cells. In any case, the impact of PB2 on the structure of PA is likely negligible because PB2 has not been shown to directly interact with PA (Digard et al., 1989; St Angelo et al., 1987; Toyoda et al., 1996). Moreover, we speculate that the observation of rapid PB1 degradation in the context of the PA–PB1 dimeric complex implies that PB1 may adopt an extended conformation in the absence of PB2 or the conserved 5′ vRNA terminal motif. It has been reported that the binding of the 5′ vRNA terminal motif to PB1 is required for

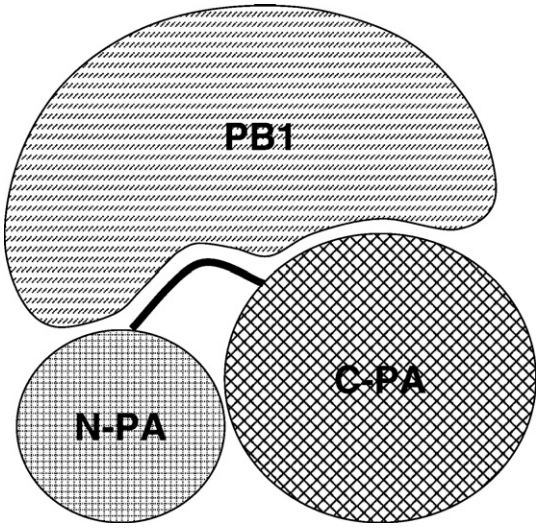

Fig. 7. Model for PA–PB1 assembly. The diagram shows a proposed complex between PA and PB1, emphasizing the two-domain structure of PA and the key role of the linker region between the domains.

polymerase activation (Gonzalez and Ortin, 1999; Li et al., 1998) and thus may stabilize PB1.

Our studies have provided a fresh glimpse into the molecular and structural anatomy of PA, its interaction with PB1, and the assembly of the influenza polymerase in general. These findings may offer new insights into previously conducted genetic studies. For example, the attenuation or loss of polymerase activities resulting from certain PA mutations may be attributed by the disruption of polymerase assembly. Information on the domain structure of the polymerase will facilitate future structural studies by identifying suitable targets for crystallization. In addition, delineation of the molecular interactions involved in polymerase assembly may have significant impact on the development of antiviral drugs, as inhibiting polymerase assembly can lead to disruption of the vital replication and transcription processes of the influenza virus.

Materials and methods

Cloning, expression, and purification

PA, PA residues 1–256 (N-PA), PA residues 277–716 (C-PA), and the PB1 coding regions from A/Puerto Rico/8/34 were cloned into pFastBac1 (Invitrogen). A six-residue histidine tag was added to the C-terminus of PA, N-PA, and C-PA. The PB1 construct was non-tagged. Generation of recombinant baculoviruses was performed according to the protocol provided with the Bac-to-Bac® Baculovirus Expression System (Version D, Invitrogen). PA, N-PA, C-PA, and PB1 were expressed by infecting Sf21 insect cells with recombinant baculoviruses at a multiplicity of infection (MOI) of 5. Infected insect cells were harvested 48 h post-infection. Cell pellets were sonicated in lysis buffer containing 50 mM Tris–HCl, pH 7.5, 300 mM NaCl, 5 mM imidazole, 10% glycerol, 17 μg/ml PMSF, 1 μg/ml leupeptin, 1 μg/ml pepstatin, and 5 mM β-mercaptoethanol. The lysate was separated by centrifugation at 25,000 ×g for 30 min. Recombinant PA, N-PA, and C-PA were purified by Ni-NTA affinity (Qiagen), heparin affinity, Superdex-200 gel filtration, and Hi-Trap Q anion exchange columns (GE). Similar protocols were followed for the expression and purification of the PA–PB1 complex, except a Hi-Trap SP cation exchange rather than a Hi-Trap Q column was employed. Purified recombinant proteins were at least 95% pure according to Coomassie SDS-PAGE.

Limited proteolysis and N-terminal sequencing

Our preliminary studies showed that 750:1 PA-to-trypsin and 250:1 PA-to-chymotrypsin mass ratios were appropriate for protease digestion studies. 1.5 mg C-His tagged PA was incubated with 0.002 mg trypsin or 0.006 mg chymotrypsin, respectively, at 20 °C for 3, 7, 15, and 25 min. Digestion was terminated by boiling at 95 °C for 5 min in an equal volume of SDS sample buffer (100 mM Tris–HCl, pH 6.8, 20% glycerol, 0.4% SDS, 0.001% bromophenol blue). Digested samples were resolved by 9% SDS-PAGE. Similar procedures were followed for chymotrypsin and trypsin digestion of PA–PB1. For Western blot analysis, digested samples were resolved by 10% SDS/PAGE and transferred to PVDF membrane (Pall). Anti-tetra His (Qiagen) was used as primary antibody to detect the six-histidine tag at the C-terminus of PA. Secondary antibodies included goat anti-chicken (Kirkegaard & Perry Lab), anti-Rabbit (Pierce), and anti-mouse (Calbiochem). Results were visualized by Fast BCIP/NBT stain (Sigma). To identify the PA fragments produced from protease digestion, two major truncated fragments were analyzed by Edman degradation at the Tufts Core Facility. Following the 40 min trypsin digestion, the 56 kD band was nearly digested, leaving the 51 kD band as the predominant band (Fig. 1B, left panel). The digested sample from 1 h of chymotrypsin digestion (Fig. 1B, right panel) was heavily loaded to produce the 45 kD fragment for N-terminal sequencing.

Far-UV circular dichroism (CD) spectroscopy

Far-UV CD spectra of purified PA, N-PA, and C-PA (2.6, 5.65, and 1.48 μM, respectively, in 10 mM phosphate, 10 mM NaCl, pH 7.5) were measured using a Jasco J-810 spectropolarimeter (1 mm path length, 20 °C). Wavelength scans were recorded from 195 to 250 nm and were averaged over eight consecutive scans (0.5 nm increment, 1 s response time, 2 nm bandwidth, 100 nm/min scanning speed). The concentrations of PA, N-PA, and C-PA were normalized to 1 μM for comparison (Fig. 3). For secondary structure prediction, algorithms available on the DICHROWEB website (Lobley et al., 2002; Whitmore and Wallace, 2004) were used to analyze CD spectra of PA, N-PA, and C-PA. Goodness of the fit was based on the parameter NRMSD (Mao et al., 1982) and best score was provided by the algorithm CDSSTR (Manavalan and Johnson, 1987).

Thermal denaturation

PA, N-PA, or C-PA (1.78, 8.2, and 8.5 μM, respectively in 25 mM phosphate, 200 mM NaCl, pH 7.5) was placed in a 1 mm path length cell and gradually heated from 25 to 95 °C at a rate of 0.5 °C per minute in the Jasco J-810, which was regulated by a Peltier temperature control system (Jasco PTC-423S). Structural changes as a function of temperature were monitored at 220 nm. The CD signal was measured every 0.5 °C (60 s delay time, 16 s response time, 3 nm bandwidth). During the course of thermal denaturation, the full spectra of protein samples were recorded from 195 to 280 nm of every 5 °C increment (1 s response time, 2 nm bandwidth, 100 nm/min scanning speed, 10 s delay time, 0.5 nm data pitch, averaged over two consecutive scans). Thermal denaturation of all protein samples is irreversible; therefore, all experiments were performed under the exact same conditions and parameters, allowing reliable comparison among the different samples on a relative scale.

Pull-down assay

Co-expression of PA, N-PA, C-PA, and PB1 was performed by co-infecting 250 ml or 1 L of Sf21 insect cells with different combinations of recombinant baculovirus at an MOI of 5 (Fig. 5A). Infected insect cells were harvested 48 h post-infection. Cell pellets were lysed and separated by centrifugation at 25,000 ×g for 30 min. The supernatant portion of the lysate was incubated with Ni-NTA resin (Qiagen) for 1 h at 4 °C. Subsequently, flowthrough (with 5 mM imidazole), wash (with 20 mM imidazole), and eluted (with 250 mM imidazole) fractions of the Ni-NTA affinity column were collected. 10 μl aliquots of each fraction were resolved by 10% SDS-PAGE and transferred to PVDF membrane for Western blot analysis. Both anti-tetra His antibody (Qiagen) and anti-PB1 antibody were used as primary antibodies to detect the presence of PA and PB1 in these fractions. Secondary antibodies included goat anti-chicken (Kirkegaard & Perry Lab), anti-Rabbit (Pierce), and anti-mouse (Calbiochem). Results were visualized by Fast BCIP/NBT stain (Sigma).

Acknowledgments

We thank Qiaozhen Ye for her preliminary work on the project and for constructing some of the recombinant baculoviruses, Erik Sedlak for assisting with secondary structure prediction, Robert Krug for providing the cDNA clones and anti-PB1 antibody, and Jon DeGnore at Tufts Core Facility for his generous help with the mass spectrometry analysis. We also thank Ying Liu, Zhao Huang, and Sarah Bondos for supplying Ultrabithorax proteins to serve as the negative control for our protease digestion experiments. We express our gratitude to Faiza Hussain, Kevin MacKenzie, Adina Maximciuc, Erik Sedlak, Yousif Shamoo, Qiaozhen Ye, and especially Douglas Mata, for critical appraisal of the manuscript. This work is supported by National

Institutes of Health (1R21AI065733 to YJT) and the Robert W. Welch Foundation (C-1588 to PWS and C-1565 to YJT).

References

Area, E., Martin-Benito, J., Gastaminza, P., Torreira, E., Valpuesta, J.M., Carrascosa, J.L., Ortin, J., 2004. 3D structure of the influenza virus polymerase complex: localization of subunit domains. Proc. Natl. Acad. Sci. U. S. A. 101 (1), 308–313.

Argos, P., 1988. A sequence motif in many polymerases. Nucleic Acids Res. 16 (21), 9909–9916.

Biswas, S.K., Nayak, D.P., 1994. Mutational analysis of the conserved motifs of influenza A virus polymerase basic protein 1. J. Virol. 68 (3), 1819–1826.

Braam, J., Ulmanen, I., Krug, R.M., 1983. Molecular model of a eucaryotic transcription complex: functions and movements of influenza P proteins during capped RNA-primed transcription. Cell 34 (2), 609–618.

Chen, W., Calvo, P.A., Malide, D., Gibbs, J., Schubert, U., Bacik, I., Basta, S., O'Neill, R., Schickli, J., Palese, P., Henklein, P., Bennink, J.R., Yewdell, J.W., 2001. A novel influenza A virus mitochondrial protein that induces cell death. Nat. Med. 7 (12), 1306–1312.

Deng, T., Sharps, J., Fodor, E., Brownlee, G.G., 2005. In vitro assembly of PB2 with a PB1–PA dimer supports a new model of assembly of influenza A virus polymerase subunits into a functional trimeric complex. J. Virol. 79 (13), 8669–8674.

Digard, P., Blok, V.C., Inglis, S.C., 1989. Complex formation between influenza virus polymerase proteins expressed in *Xenopus* oocytes. Virology 171 (1), 162–169.

Fechter, P., Mingay, L., Sharps, J., Chambers, A., Fodor, E., Brownlee, G.G., 2003. Two aromatic residues in the PB2 subunit of influenza A RNA polymerase are crucial for cap binding. J. Biol. Chem. 278 (22), 20381–20388.

Fodor, E., Crow, M., Mingay, L.J., Deng, T., Sharps, J., Fechter, P., Brownlee, G.G., 2002. A single amino acid mutation in the PA subunit of the influenza virus RNA polymerase inhibits endonucleolytic cleavage of capped RNAs. J. Virol. 76 (18), 8989–9001.

Fodor, E., Mingay, L.J., Crow, M., Deng, T., Brownlee, G.G., 2003. A single amino acid mutation in the PA subunit of the influenza virus RNA polymerase promotes the generation of defective interfering RNAs. J. Virol. 77 (8), 5017–5020.

Fodor, E., Seong, B.L., Brownlee, G.G., 1993. Photochemical cross-linking of influenza A polymerase to its virion RNA promoter defines a polymerase binding site at residues 9 to 12 of the promoter. J. Gen. Virol. 74 (Pt 7), 1327–1333.

Fodor, E., Smith, M., 2004. The PA subunit is required for efficient nuclear accumulation of the PB1 subunit of the influenza A virus RNA polymerase complex. J. Virol. 78 (17), 9144–9153.

Ghanem, A., Mayer, D., Chase, G., Tegge, W., Frank, R., Kochs, G., Garcia-Sastre, A., Schwemmle, M., 2007. Peptide-mediated interference with influenza A virus polymerase. J. Virol. 81 (14), 7801–7804.

Gonzalez, S., Ortin, J., 1999. Distinct regions of influenza virus PB1 polymerase subunit recognize vRNA and cRNA templates. EMBO J. 18 (13), 3767–3775.

Gonzalez, S., Zurcher, T., Ortin, J., 1996. Identification of two separate domains in the influenza virus PB1 protein involved in the interaction with the PB2 and PA subunits: a model for the viral RNA polymerase structure. Nucleic Acids Res. 24 (22), 4456–4463.

Hara, K., Schmidt, F.I., Crow, M., Brownlee, G.G., 2006. Amino acid residues in the N-terminal region of the PA subunit of influenza A virus RNA polymerase play a critical role in protein stability, endonuclease activity, cap binding, and virion RNA promoter binding. J. Virol. 80 (16), 7789–7798.

Hara, K., Shiota, M., Kido, H., Ohtsu, Y., Kashiwagi, T., Iwahashi, J., Hamada, N., Mizoue, K., Tsumura, N., Kato, H., Toyoda, T., 2001. Influenza virus RNA polymerase PA subunit is a novel serine protease with Ser624 at the active site. Genes Cells 6 (2), 87–97.

Honda, A., Mizumoto, K., Ishihama, A., 2002. Minimum molecular architectures for transcription and replication of the influenza virus. Proc. Natl. Acad. Sci. U. S. A. 99 (20), 13166–13171.

Huarte, M., Falcon, A., Nakaya, Y., Ortin, J., Garcia-Sastre, A., Nieto, A., 2003. Threonine 157 of influenza virus PA polymerase subunit modulates RNA replication in infectious viruses. J. Virol. 77 (10), 6007–6013.

Jones, D.T., 1999. Protein secondary structure prediction based on position-specific scoring matrices. J. Mol. Biol. 292 (2), 195–202.

Kawaguchi, A., Naito, T., Nagata, K., 2005. Involvement of influenza virus PA subunit in assembly of functional RNA polymerase complexes. J. Virol. 79 (2), 732–744.

Kobayashi, M., Toyoda, T., Ishihama, A., 1996. Influenza virus PB1 protein is the minimal and essential subunit of RNA polymerase. Arch. Virol. 141 (3–4), 525–539.

Lamb, R.A., Krug, R.M., 2001. *Orthomyxoviridae*: the viruses and their replication, In: Knipe, D.M., Howley, P.M. (Eds.), 4 ed. Fields Virology, Vol. 1. Lippincott-Raven, pp. 1487–1531. 2 vols.

Lee, M.T., Bishop, K., Medcalf, L., Elton, D., Digard, P., Tiley, L., 2002. Definition of the minimal viral components required for the initiation of unprimed RNA synthesis by influenza virus RNA polymerase. Nucleic Acids Res. 30 (2), 429–438.

Li, M.L., Ramirez, B.C., Krug, R.M., 1998. RNA-dependent activation of primer RNA production by influenza virus polymerase: different regions of the same protein subunit constitute the two required RNA-binding sites. EMBO J. 17 (19), 5844–5852.

Li, M.L., Rao, P., Krug, R.M., 2001. The active sites of the influenza cap-dependent endonuclease are on different polymerase subunits. EMBO J. 20 (8), 2078–2086.

Lobley, A., Whitmore, L., Wallace, B.A., 2002. DICHROWEB: an interactive website for the analysis of protein secondary structure from circular dichroism spectra. Bioinformatics 18 (1), 211–212.

Manavalan, P., Johnson Jr., W.C., 1987. Variable selection method improves the prediction of protein secondary structure from circular dichroism spectra. Anal. Biochem. 167 (1), 76–85.

Mao, D., Wachter, E., Wallace, B.A., 1982. Folding of the mitochondrial proton adenosinetriphosphatase proteolipid channel in phospholipid vesicles. Biochemistry 21 (20), 4960–4968.

Meiler, J., Baker, D., 2003. Coupled prediction of protein secondary and tertiary structure. Proc. Natl. Acad. Sci. U. S. A. 100 (21), 12105–12110.

Meiler, J., Müller, M., Zeidler, A., Schmäschke, F., 2001. Generation and evaluation of dimension-reduced amino acid parameter representations by artificial neural networks. J. Mol. Model. 7 (9), 360–369.

Miyazaki, S., Kuroda, Y., Yokoyama, S., 2002. Characterization and prediction of linker sequences of multi-domain proteins by a neural network. J. Struct. Funct. Genomics 2 (1), 37–51.

Naffakh, N., Massin, P., van der Werf, S., 2001. The transcription/replication activity of the polymerase of influenza A viruses is not correlated with the level of proteolysis induced by the PA subunit. Virology 285 (2), 244–252.

Nakagawa, Y., Oda, K., Nakada, S., 1996. The PB1 subunit alone can catalyze cRNA synthesis, and the PA subunit in addition to the PB1 subunit is required for viral RNA synthesis in replication of the influenza virus genome. J. Virol. 70 (9), 6390–6394.

Nieto, A., de la Luna, S., Barcena, J., Portela, A., Ortin, J., 1994. Complex structure of the nuclear translocation signal of influenza virus polymerase PA subunit. J. Gen. Virol. 75 (Pt 1), 29–36.

Ohtsu, Y., Honda, Y., Sakata, Y., Kato, H., Toyoda, T., 2002. Fine mapping of the subunit binding sites of influenza virus RNA polymerase. Microbiol. Immunol. 46 (3), 167–175.

Perales, B., Sanz-Ezquerro, J.J., Gastaminza, P., Ortega, J., Santaren, J.F., Ortin, J., Nieto, A., 2000. The replication activity of influenza virus polymerase is linked to the capacity of the PA subunit to induce proteolysis. J. Virol. 74 (3), 1307–1312.

Perez, D.R., Donis, R.O., 1995. A 48-amino-acid region of influenza A virus PB1 protein is sufficient for complex formation with PA. J. Virol. 69 (11), 6932–6939.

Perez, D.R., Donis, R.O., 2001. Functional analysis of PA binding by influenza a virus PB1: effects on polymerase activity and viral infectivity. J. Virol. 75 (17), 8127–8136.

Pollastri, G., McLysaght, A., 2005. Porter: a new, accurate server for protein secondary structure prediction. Bioinformatics 21 (8), 1719–1720.

Pollastri, G., Przybylski, D., Rost, B., Baldi, P., 2002. Improving the prediction of protein secondary structure in three and eight classes using recurrent neural networks and profiles. Proteins 47 (2), 228–235.

Raghava, G.P.S., 2002. APSSP2: a combination method for protein secondary structure prediction based on neural network and example based learning. CASP 5, A-132.

Regan, J.F., Liang, Y., Parslow, T.G., 2006. Defective assembly of influenza A virus due to a mutation in the polymerase subunit PA. J. Virol. 80 (1), 252–261.

Sanz-Ezquerro, J.J., de la Luna, S., Ortin, J., Nieto, A., 1995. Individual expression of influenza virus PA protein induces degradation of coexpressed proteins. J. Virol. 69 (4), 2420–2426.

Sanz-Ezquerro, J.J., Fernandez Santaren, J., Sierra, T., Aragon, T., Ortega, J., Ortin, J., Smith, G.L., Nieto, A., 1998. The PA influenza virus polymerase subunit is a phosphorylated protein. J. Gen. Virol. 79 (Pt 3), 471–478.

Sanz-Ezquerro, J.J., Zurcher, T., de la Luna, S., Ortin, J., Nieto, A., 1996. The amino-terminal one-third of the influenza virus PA protein is responsible for the induction of proteolysis. J. Virol. 70 (3), 1905–1911.

St Angelo, C., Smith, G.E., Summers, M.D., Krug, R.M., 1987. Two of the three influenza viral polymerase proteins expressed by using baculovirus vectors form a complex in insect cells. J. Virol. 61 (2), 361–365.

Suyama, M., Ohara, O., 2003. DomCut: prediction of inter-domain linker regions in amino acid sequences. Bioinformatics 19 (5), 673–674.

Tanaka, T., Yokoyama, S., Kuroda, Y., 2006. Improvement of domain linker prediction by incorporating loop-length-dependent characteristics. Biopolymers 84 (2), 161–168.

Toyoda, T., Adyshev, D.M., Kobayashi, M., Iwata, A., Ishihama, A., 1996. Molecular assembly of the influenza virus RNA polymerase: determination of the subunit–subunit contact sites. J. Gen. Virol. 77 (Pt 9), 2149–2157.

Whitmore, L., Wallace, B.A., 2004. DICHROWEB, an online server for protein secondary structure analyses from circular dichroism spectroscopic data. Nucleic Acids Res. 32 (Web Server issue), W668–W673.

Whittaker, G.R., 2001. Intracellular trafficking of influenza virus: clinical implications for molecular medicine. Expert Rev. Mol. Med. 2001, 1–13.

Zurcher, T., de la Luna, S., Sanz-Ezquerro, J.J., Nieto, A., Ortin, J., 1996. Mutational analysis of the influenza virus A/Victoria/3/75 PA protein: studies of interaction with PB1 protein and identification of a dominant negative mutant. J. Gen. Virol. 77 (Pt 8), 1745–1749.